Bioconjugate Chemistry

Communication

pubs.acs.org/bc

Cascade Biocatalysis by Multienzyme−Nanoparticle Assemblies

Wei Kang,[†] Jiahui Liu,[†] Jianpeng Wang,[†] Yunyu Nie,[†] Zhihong Guo,[‡] and Jiang Xia*[,†]

[†]Department of Chemistry, The Chinese University of Hong Kong, Shatin, Hong Kong SAR, China

[‡]Department of Chemistry, The Hong Kong University of Science and Technology, Clear Water Bay, Kowloon, Hong Kong SAR, China

Supporting Information

ABSTRACT: Multienzyme complexes are of paramount importance in biosynthesis in cells. Yet, how sequential enzymes of cascade catalytic reactions synergize their activities through spatial organization remains elusive. Recent development of site-specific protein−nanoparticle conjugation techniques enables us to construct multienzyme assemblies using nanoparticles as the template. Sequential enzymes in menaquinone biosynthetic pathway were conjugated to CdSe-ZnS quantum dots (QDs, a nanosized particulate material) through metal-affinity driven self-assembly. The assemblies were characterized by electrophoretic methods, the catalytic activities were monitored by reverse-phase chromatography, and the composition of the multienzyme−QD assemblies was optimized through a progressive approach to achieve highly efficient catalytic conversion. Shorter enzyme−enzyme distance was discovered to facilitate intermediate transfer, and a fine control on the stoichiometric ratio of the assembly was found to be critical for the maximal synergy between the enzymes. Multienzyme−QD assemblies thereby provide an effective model to scrutinize the synergy of cascade enzymes in multienzyme complexes.

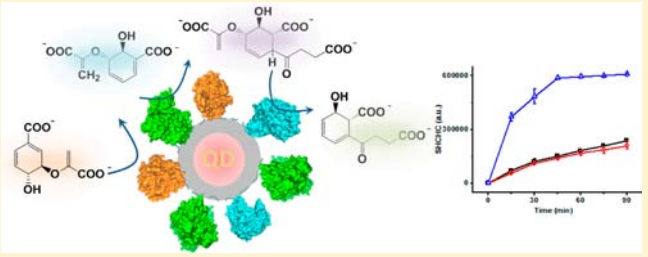

INTRODUCTION

Multienzyme complexes are prevalent nanomachines in nature that catalyze enzymatic conversions of sequential reactions. In these complexes, cascade enzymes, each dedicated to a single catalytic activity in sequential chemical conversions, are often assembled into sophisticated three-dimensional structures with nanosizes and well-controlled geometries.[1−5] Representative examples of multienzyme nanomachines are cellulosomes, which contain multiple catalytic modules assembled on the protein scaffolding which orchestrate the deconstruction of cellulose and hemicellulose.[6,7] Spatial proximity synergizes the activities of cascade enzymes, which is manifested by the elevation of the overall efficiency of substrate catalysis and product generation as well as a fine-control of the intermediate flux. Intrigued by nature's design of multienzyme architectures, chemists and metabolic engineers construct artificial multienzyme complexes by harnessing specific and noncovalent biorecognitions.[8−15] For example, cascade enzymes have been assembled on artificial scaffolding or synthetic scaffold proteins through protein−protein interactions,[16−19] on DNA templates through protein−DNA interactions,[20−23] on chemical scaffolds through bioconjugation reactions,[24−26] or alternatively, enzyme proximity has been realized by physical compartmentalization.[27,28]

Nanoparticles can also serve as a valid template for protein assembly. In particular, CdSe−ZnS core/shell quantum dots (QDs) with diameter ranging 3−5 nm can site-specifically bind to proteins and form larger nanosized assemblies with a protein corona resembling multienzyme complexes.[29−37] Through the high-affinity metal−hexahistidine peptide interaction, around 16 to 20 histagged enzymes can bind to and cover the surface of QDs in a programmable manner under physiological condition.[38−42] The protein−QD assemblies remain soluble as monodisperse nanoparticles in solution, are highly stable for a considerably long period of time, and can resist the displacement of competing molecules.[41,42] The special properties of metal-affinity driven assembly then intrigued us to investigate the use of QDs as the core to assemble cascade enzymes; the multienzyme−QD assemblies will allow us to simulate natural multienzyme complexes and to investigate how spatial organization affects cascade catalysis (Figure 1A). Here we chose menaquinone biosynthetic enzymes for assembly. Menaquinones, a.k.a. vitamin K2, are a group of molecules with a common 2-methyl-1,4-naphthoquinone structure.[43,44] In *E. coli*, a series of enzymes, collectively called menaquinone biosynthetic enzymes, are responsible for the synthesis of menaquinone (Figure 1B). The first enzyme, MenF, isomerizes chorismate to isochorismate,[45,46] and MenD (dependent on thiamine diphosphate coenzyme) catalyzes a Stetter-like conjugate addition of α-ketoglutarate with isochorismate to form 2-succinyl-5-enolpyruvyl-6-hydroxy-3-cyclohexadiene-1-carboxylate, SEPHCHC.[47,48] SEPHCHC then undergoes pyruvate elimination catalyzed by MenH to give 2-succinyl-6-hydroxy-2,4-cyclo-hexadiene-1-carboxylate, SHCHC,[49,50] which

Received: June 1, 2014
Revised: July 11, 2014
Published: July 14, 2014

   dx.doi.org/10.1021/bc5002399 | *Bioconjugate Chem.* 2014, 25, 1387−1394

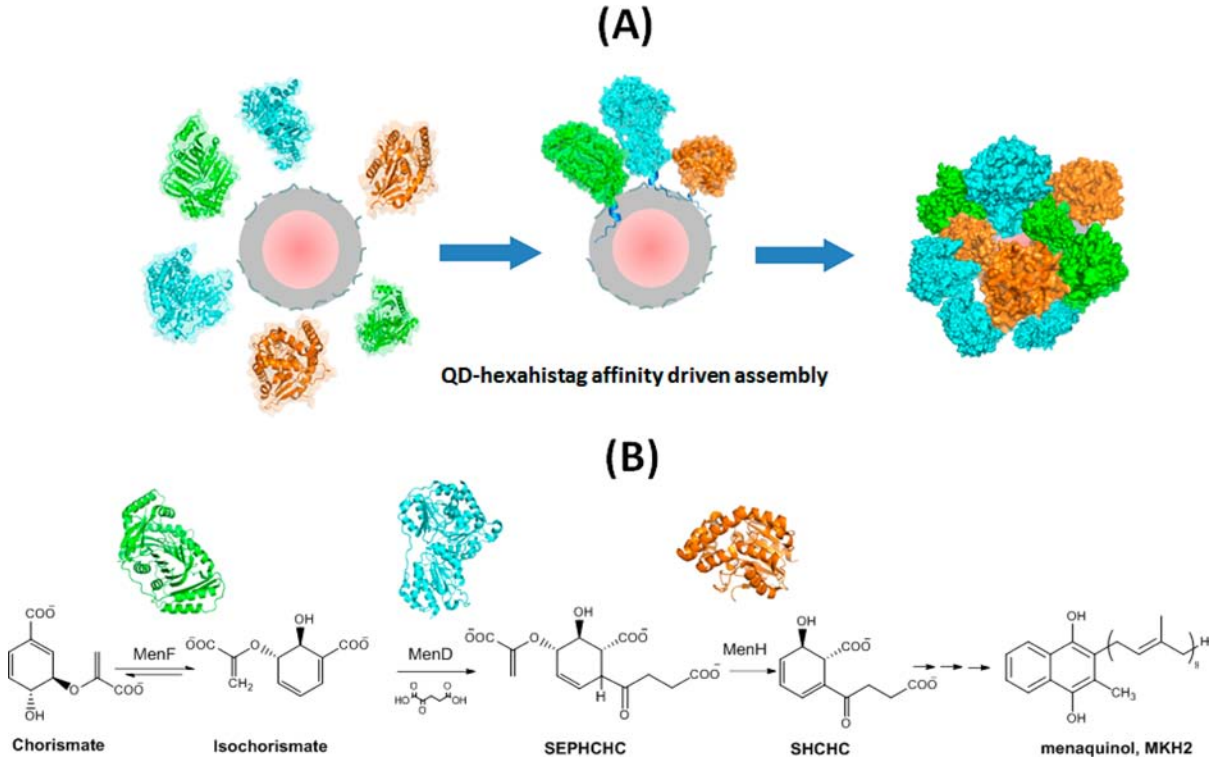

Figure 1. Construction of multienzyme−QD assemblies to mimic multienzyme complexes. (A) QD-hexahistag affinity drives the site-specific assembly of enzymes on the surface of QDs. (B) Cascade enzymes in menaquinone synthetic pathway catalyze sequential conversion of chorismate. The structures of MenF, MenD, and MenH were drawn based on their crystal structures (PDB IDs 2EUA, 2JLC, and 2XMZ)[51−54] and color coded, respectively.

finally leads to menaquinol through several additional enzymatic steps. MenF, MenD, and MenH are particularly suitable candidates for multienzyme assemblies. First, they have been expressed as soluble proteins through recombinant technology, and their crystal structures are all available.[51−54] Also there is no interaction between the three enzymes in solution (see Supporting Information for details). Second, the substrate, intermediates, and products (i.e., chorismate, isochorismate, and SHCHC) have distinct retention times in reverse-phase HPLC.[45−50] Also important, these molecules carry negative charges which abolishes any nonspecific interaction with the negatively charged surface of ZnS-CdSe QDs. Therefore, we recombinantly expressed MenF, MenD, and MenH and assembled them with QDs through metal-histag affinity driven self-assembly to probe how cascade enzymes work synergistically as a nanoparticle assembly (Figure 1).

RESULTS AND DISCUSSION

Programmable Assembly of Enzymes on QDs. MenF, MenD, and MenH carrying hexahistidine tags (i.e., histags) were cloned, expressed, and purified to homogeneity (Figures S1 and S2 and experimental details can be found in the Supporting Information).[45−54] Histag was fused at the N termini of all the enzymes, because this position is distant from the active site based on their crystal structures (Supporting Information Figure S3).[51−54] We then examined the formation of enzyme−QD assemblies between the purified MenF, MenD, and MenH and CdSe-ZnS QDs. Oligohistidine has been shown to bind to the surface of glutathione-stabilized CdSe-ZnS core/shell QDs with high affinity and specificity by displacing surface-bound glutathione molecules.[41,42,55,56] Through this ligand exchange process, histagged fluorescent proteins and functional receptors have been stably presented on the surface of QDs without loss of function.[29,31,41,42] We and others have demonstrated that statistically a QD nanoparticle can accommodate 16 to 20 protein molecules on its surface.[38−43] To confirm the capability of QDs in accommodating the menaquinone biosynthetic enzymes, we incubated CdSe-ZnS QDs (having a diameter of 3.5 nm and maximal emission wavelength of 565 nm) and enzymes in 5- to 20-fold molar excess and then analyzed by electrophoresis. Agarose gel electrophoresis could resolve enzyme−QD complexes from the free QDs as enzyme−QD assemblies migrate much more slowly than free QDs in gel. The mobility of the assemblies correlated with the average number of proteins per QD particle; increasing stoichiometry n of the protein in $(\text{protein})_n$−QD assembly leads to correspondingly slower mobility. We have observed that when the ratio of enzyme to QDs reached 15:1, further increase of the enzyme/QD ratio (e.g., higher than 20:1) did not cause a shift of the QD-enzyme band, indicating that the surface of QDs reached saturation at enzyme/QD molar ratio above 15:1 (Figure 2). Staining the agarose gel with Coomassie dye verified that at protein/QD molar ratio below 15:1, all the enzymes are involved in assembly formation under this condition (therefore, the only enzyme species in the solution is enzyme−QD assemblies) (Supporting Information Figure S4). Notably, the assembly of a heterologous mixture of the enzymes on QDs followed the same saturation trend. When MenF and MenD at equimolar ratio were mixed with QDs, saturation was also observed at the stoichiometry of total protein (MenF + MenD) above 15. The same trend was also observed in the three-enzyme assembly system (MenF + MenD + MenH + QDs) (Supporting

dx.doi.org/10.1021/bc5002399 | Bioconjugate Chem. 2014, 25, 1387−1394

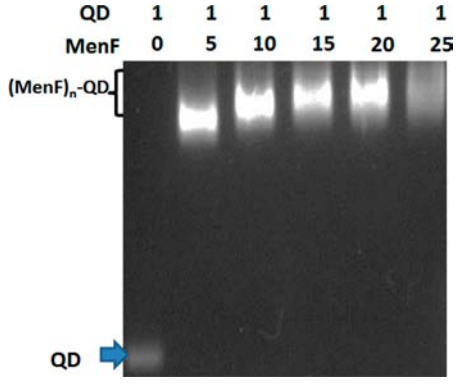

Figure 2. Enzyme–QD assembly probed by agarose electrophoresis. His-tagged MenF enzyme was incubated with QDs at indicated ratios to give the assemblies, and the assemblies were resolved in agarose gel by electrophoresis at 4 °C and imaged under UV. $(MenF)_{25}$-QD assembly showed similar mobility as $(MenF)_{20}$-QD assembly, indicating that saturation of surface binding sites of QDs was achieved at 20:1 ratio.

Information Figure S5). Therefore, consistent with previous reports,[38−42] a QD (3.5 nm in diameter) can accommodate at least 15 enzyme molecules, despite that the enzymes are different in size and electrostatic property. In the following study a maximum ratio of 15:1 was then used for multienzyme–QD assembly. Capillary electrophoresis coupled with fluorescence detection (CE-FL) was employed to verify the dispersity and solubility of the particulate assemblies (Supporting Information Figure S6).[55] The mobility of enzyme–QD species changes with increasing enzyme/QD ratio, and no precipitation was observed in CE-FL (Supporting Information Figure S7).

HPLC Monitoring of the Reaction Progress. The substrates and products involved in MenF, MenH, and MenD catalyzed reactions (i.e., chorismate, isochorismate, and SHCHC) can be well resolved on reverse-phase HPLC due to their different retention times on C18 column.[45−50] Chorismate, isochorismate, and SHCHC were eluted at 8.52, 7.83, and 4.20 min, respectively (Figure 3). The product of MenD, SEPHCHC, does not have absorption at UV–vis range, precluding it from direct monitoring by HPLC. But it is known

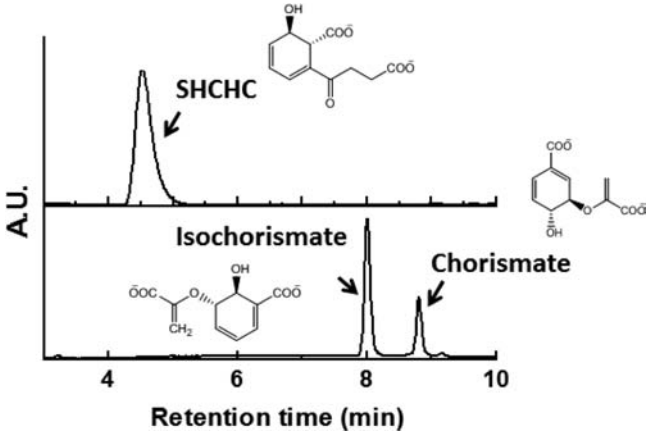

Figure 3. HPLC separation of chorismate, isochorismate, and SHCHC. The detection wavelength of chorismate and isochorismate was set to 278 nm, and the detection wavelength of SHCHC was set at 290 nm.

though that through alkaline treatment, SEPHCHC can be quantitatively converted to SHCHC, which can be visualized on HPLC at 290 nm.[47] We then utilized this treatment to monitor the reaction from isochorismate to SEPHCHC catalyzed by MenD.

Enzyme–QD Assembly v Free Enzymes. We next set out to examine the catalytic activity of enzyme–QD assemblies. Initially, we fixed the enzyme to QD molar ratio to 5:1. MenF catalyzes the conversion of chorismate to isochorismate, which reaches equilibrium with an isochorismate/chorismate ratio around 3:1. MenF–QD assemblies **1b** (5:1 ratio) showed a similar reaction rate to free MenF **1a** with apparent rate k_{app} values measured at 0.11 min^{-1} and 0.12 min^{-1} respectively (Figure 4A). As **1a** and **1b** contain the same amount of enzyme MenF, this indicates that complexation with QDs did not affect the catalytic activity of MenF. Similarly, site specific conjugation with QDs did not affect the catalytic activity of MenD and MenH (Supporting Information Figure S8). We then mixed two enzymes MenF and MenD with QDs to form bienzyme–QD assemblies. As MenD converts isochorismate (the product of MenF) to SEPHCHC nonreversibly, we assembled MenF and MenD at 1:1 ratio on QDs (**2b**) with a final total protein-to-QD ratio of 5:1 (or MenF/MenD/QDs = 2.5:2.5:1). Aliquots were taken every 15 min, the reactions were stopped, the product SEPHCHC was quantitatively converted to SHCHC through alkaline treatment, and the amount of SHCHC was then quantified by HPLC to indicate the quantity of the product SEPHCHC. We observed that MenF/MenD bienzyme–QD assemblies **2b** showed slower product conversion than free enzymes in solution (**2a**) (Figure 4B). The same trend was also observed in trienzyme system including MenF, MenD, and MenH (MenF/MenD/MenH/QDs = 1.67:1.67:1.67:1; total protein-to-QD ratio also set to 5:1). MenF converts chorismate to isochorismate; MenD converts isochorismate to SEPHCHC and finally to SHCHC by MenH. Trienzyme–QD assembly (**3b**) showed a slower conversion of chorismate to SHCHC than free enzymes **3a** in solution (Figure 4C). We reasoned that intermediate transportation limited chemical conversion in cascade reactions of multienzyme assemblies. At 5:1 protein-to-QD ratio, assuming the out-layer of the assemblies has a diameter of 5 nm and each QD has an average of 5 proteins, the distance between the active sites can be estimated to be around 8 nm (Supporting Information Figure S9). For reactions catalyzed by free enzymes in solution, intermediate molecules diffuse between the protein entities driven by Brownian motion to reach the next catalytic site. In multienzyme complexes, besides interassembly diffusion (the assemblies, 100 times larger than single proteins, will deter interassembly diffusion), intermediate transportation between actives within the same assembly might be a bottleneck of the overall cascade reaction.

Shortening Enzyme–Enzyme Distance. To improve intra-assembly transportation, we sought to shorten enzyme–enzyme distance in the multienzyme–QD assemblies. Increasing enzyme-to-QD ratio will increase the density of the enzymes on the surface of QDs, which thereby lowers enzyme–enzyme distance within each assembly. We then constructed bienzyme–QD assemblies with the ratio of MenF/MenD/QD being 2.5:2.5:1 (**4a**, n = 5), 5:5:1 (**4b**, n = 10), and 7.5:7.5:1 (**4c**, n = 15), respectively (Figure 5A). The total amounts of the enzymes were kept the same while the quantities of QDs were reduced to result in higher ratios of total enzyme to QDs. Higher enzyme density, despite the same amount of the

dx.doi.org/10.1021/bc5002399 | Bioconjugate Chem. 2014, 25, 1387−1394

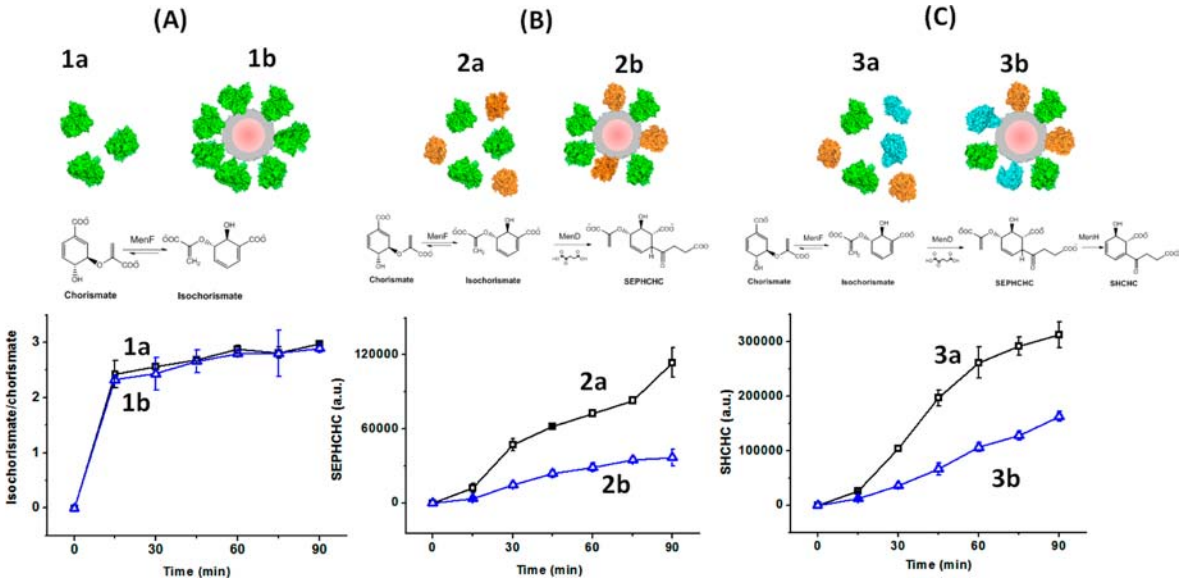

Figure 4. Enzyme−QD assemblies were catalytically active. (A) Comparison of the catalytic rate of QD-complexed MenF with that of free MenF, measured by isochorismate:chorismate ratio. (B) Comparison of the catalytic rate of QD-complexed MenF and MenD (MenF/MenD/QDs = 2.5:2.5:1) with that of free MenF and MenD mixture, measured by the production of SEPHCHC. (C) Comparison of the catalytic rate of QD-complexed MenF, MenD, and MenH (MenF/MenD/MenH/QDs = 1.67:1.67:1.67:1) with that of free MenF, MenD, and MenH mixture, measured by the production of SHCHC. The total amount of enzyme(s), volume of the reaction solution, and the initial concentration of chorismate were the same in all the experiments.

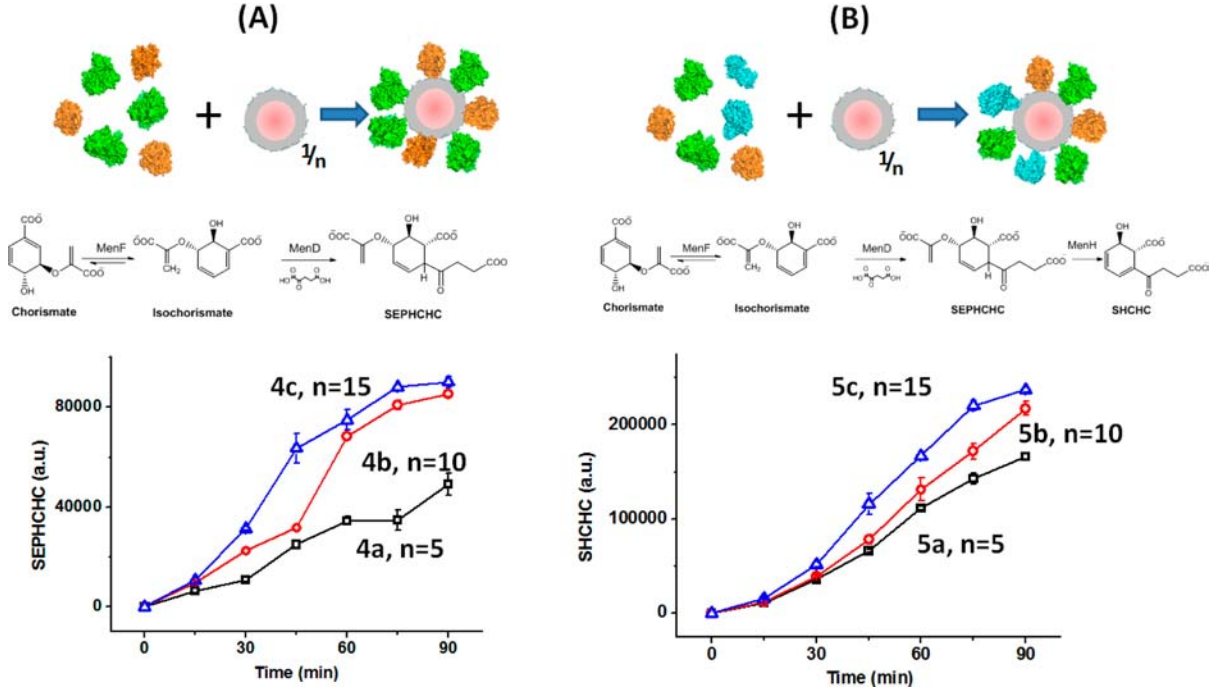

Figure 5. Catalytic efficiency of multienzyme−QD assemblies correlated with enzyme−enzyme distance. (A) MenF/MenD bienzyme−QD assemblies of low (**4a**, n = 5), intermediate (**4b**, n = 10), and high (**4c**, n = 15) density exerted increasing catalytic efficacy. The production of SEPHCHC was measured by the amount of SHCHC after quantitative conversion of SEPHCHC by an alkaline treatment. (B) MenF/MenD/MenH trienzyme−QD assemblies of low (**5a**, n = 5), intermediate (**5b**, n = 10), and high (**5c**, n = 15) density exerted increasing catalytic efficacy. In all the experiments, the total amounts of the enzymes, volumes of the reaction solutions, and the initial concentrations of chorismate were all the same; only the amounts of QDs were adjusted to result in different enzyme/QD ratios.

enzyme employed, improved the overall production of SEPHCHC with an order of **4c** > **4b** > **4a** (Figure 5A). Assuming in assembly **4a** that the distance between each active site is estimably 8 nm, in **4b** and **4c**, we estimated the interenzyme distances decreased to 5.6 and 4.6 nm, respectively (Supporting Information Figure S9). The activity increase was also observed in MenF/MenD/MenH trienzyme−QD assemblies (Figure 5B). Increasing the ratio of total enzyme to QDs from **5a** (n = 5), to **5b** (n = 10), and to **5c** (n = 15) markedly increased the production rate of SHCHC. Therefore,

dx.doi.org/10.1021/bc5002399 | *Bioconjugate Chem.* 2014, 25, 1387−1394

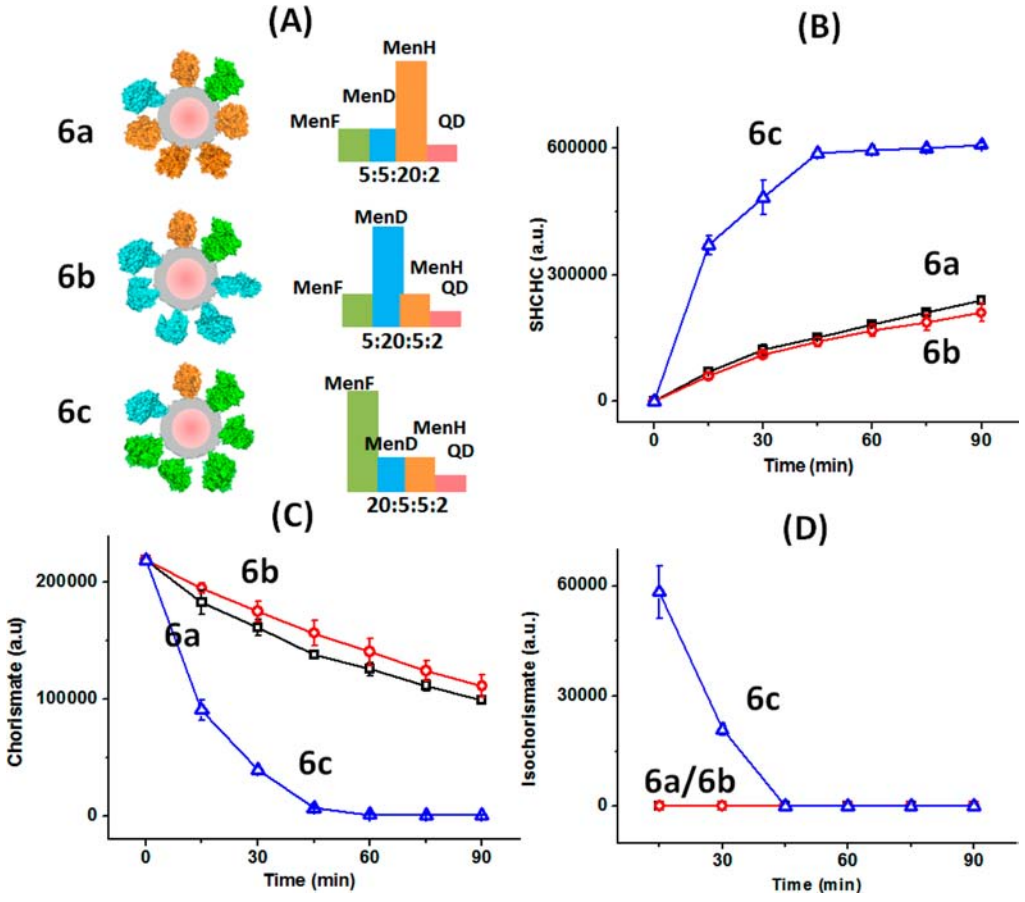

Figure 6. Composition of the enzymes in the assemblies drastically affected the catalytic efficacy and intermediate flow. (A) Schematic illustration of three multienzyme−QD assemblies with excess MenH (**6a**), MenD (**6b**), and MenF (**6c**), respectively. (B) Product (SHCHC) generation catalyzed by the three assemblies. (C) Substrate (chorismate) consumption catalyzed by the three assemblies. (D) Intermediate (isochorismate) accumulation catalyzed by the three assemblies. The total amounts of the enzymes and QDs, volumes of the reaction solutions, and the initial concentrations of chorismate were all the same in **6a**, **6b**, and **6c**.

decreasing enzyme−enzyme distances in the QD-templated assemblies facilitated the intra-assembly transfer of the product of a catalytic conversion to the next cascade enzyme. Multienzyme complexes in nature often employ the same strategy, i.e., close alignment of cascade enzymes, to assist the substrate transfer between different active sites; increasing the efficiency of production pipeline promotes the production conversion and avoids the accumulation of the intermediates in proximity to the complexes, which often poses inhibitory or toxic effects.

Controlling the Intermediate Transportation. We then adjusted the composition of the enzymes in the assemblies to achieve effective transportation of the intermediate in the cascade reaction. With the ratio of total enzyme to QD fixed at 15:1, we increased the weight of MenH, MenD, and MenF, respectively, which gave three assemblies **6a**, **6b**, and **6c** (Figure 6A). Assembly **6c**, with 4-fold excess of MenF, exhibited the highest production of SHCHC, whereas assemblies **6a** and **6b** are much slower, despite the same amount of total enzymes and QDs present in all the assemblies (Figure 6B). The apparent rate of assembly **6c** (k_{app} = 0.059 min^{-1}) is 3.5 times higher than **6a** and **6b** (0.017 and 0.016 min^{-1}, respectively). Assembly **6c** produced 4.2 times and 3.8 times more SHCHC than assemblies **6a** and **6b**, respectively, after 45 min. This was also consistent with the rapid consumption of chorismate by **6c** (Figure 6C). Chorismate was completely consumed after 45 min, which corresponded well with the time the content of SHCHC reached plateau. The clustering of MenD and MenH lead to efficient conversion of isochorismate to SEPHCHC and to SHCHC, as the production of SHCHC corresponds to the immediate consumption of chorismate. We also measured the change of the intermediate isochorismate in the three reaction systems (Figure 6D). In the case of assemblies **6a** and **6b**, there was no accumulation of isochorismate, which seemed to be rapidly converted in the downstream reactions. However, in the case of assembly **6c**, we observed a peak level of isochorismate at 15 min which declined to zero at 45 min. This indicated that 4-fold excess of MenF provided sufficient amount of isochorismate for downstream intraparticle enzymes to process in this system, and the nanomachine was functioning at its maximal potency. To further elaborate the effect of intraparticle intermediate flow versus interparticle transfer (Supporting Information Figure S10), we constructed enzyme−QD mixture systems by mixing preformed MenF−QD, MenD−QD, and MenH−QD assemblies at the same ratio as in Figure 6. The product of MenF−QD must reach MenD−QD and then MenH−QD for catalysis through interparticle transfer in mixture systems **7a**−**7c**, whereas in multienzyme assembly **6a**−**6c** both intra- and interparticle intermediate flow are possible. We observed that the substance profile catalyzed by the mixture systems markedly differed from that catalyzed by the multienzyme assemblies

dx.doi.org/10.1021/bc5002399 | *Bioconjugate Chem.* 2014, 25, 1387−1394

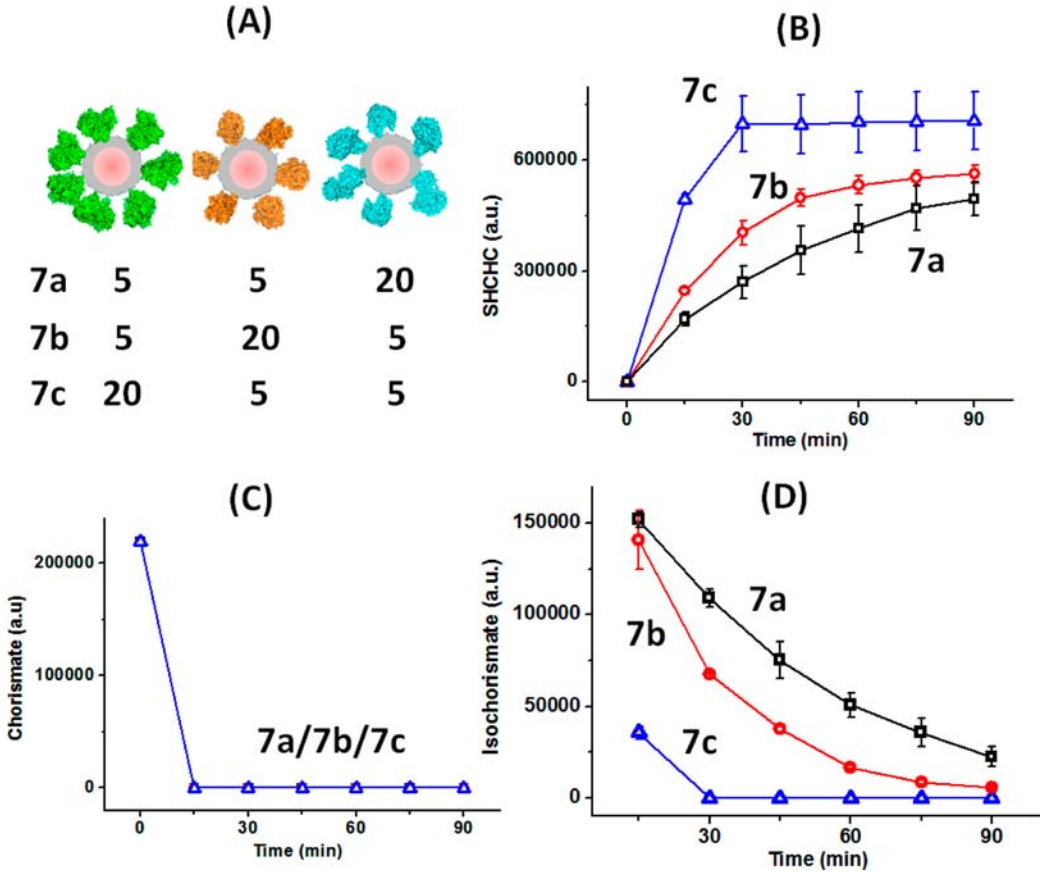

Figure 7. Profiling cascade catalysis by enzyme−QD mixture systems. (A) MenF−QD, MenD−QD, and MenH−QD assemblies were preformed and then mixed to give three mixture systems **7a**, **7b**, and **7c**. (B) Product (SHCHC) generation catalyzed by the three mixture systems. (C) Substrate (chorismate) consumption catalyzed by the three mixture systems. (D) Intermediate (isochorismate) accumulation catalyzed by the three mixture systems. The total amounts of the enzymes and QDs, volumes of the reaction solutions, and the initial concentrations of chorismate were all the same in **7a**, **7b**, and **7c**.The mixture system **7a** has identical amounts of MenF, MenD, MenH, and QDs as **6a**, and analogously **7b** as **6b**, and **7c** as **6c**.

(Figure 7), despite their identical compositions in each pair. For example, a significant amount of isochorismate accumulated in the mixture systems **7a** and **7b**, but not in the corresponding multienzyme assemblies **6a** and **6b** (Figure 7D). This suggests that intraparticle substance flow likely plays an instrumental role in multienzyme assemblies. It also suggests that forming multienzyme complexes in nature might avoid undesired buildup of intermediates, which are often toxic to the cellular environment during biosynthesis.

■ CONCLUSION

Many enzymes, in particular, those involved in catalyzing sequential chemical conversions in biosynthetic or metabolic pathways are not standalone in solution; instead, they often form clusters as multienzyme complexes to achieve a tight control on substrate consumption, intermediate flux, and production generation.[1−5] Promoting proximity of active sites that catalyze sequential chemical steps in limited space and dimension represents one common strategy that multienzyme complexes employ to speed up chemical reaction. Here we report a templated assembly of multiple copies of menaquinone biosynthetic enzymes on nanoparticle QD scaffolds enabled by site-specific assembly of histagged proteins on CdSe−ZnS QDs. By constituting multienzyme−QD assemblies with different combinations of MenF, MenD, and MenH and QDs, we manifested a progressive approach that eventually realized control on substrate consumption, intermediate accumulation, and product generation. We discovered that the catalytic efficacy of multienzyme−QD is predominantly dictated by enzyme−enzyme distance, and an appropriate stoichiometry of the enzyme assembly is critical to yield optimal intermediate transportation to facilitate the cascade catalysis.

Despite its similarity with natural complexes, multienzyme−QD assembly has its limitation. First, the QD-centered assemblies are globular in shape with all the active sites displayed on the exterior of the particle, much like the architecture of pyruvate dehydrogenase complex, but the architectures of natural multienzyme complexes are not limited to globular shape, and even include sophisticated substructures such as substrate channels and intermediate highways.[57,58] Second, protein−QD assembly allowed us to freely adjust the stoichiometry of each enzyme in the assembly, but the final ratio within each assembly is only statistical. Nevertheless, our work manifested a new use of protein−nanoparticle conjugation techniques, and provided a convenient system to investigate the clustering effect of enzymes, which nature often harnesses to achieve regulation through enzyme complexation, compartmentalization, and membrane-embedment.

dx.doi.org/10.1021/bc5002399 | *Bioconjugate Chem.* 2014, 25, 1387−1394

■ ASSOCIATED CONTENT

Supporting Information

Materials and Methods. Figures S1 to S10. This material is available free of charge via the Internet at http://pubs.acs.org.

■ AUTHOR INFORMATION

Corresponding Author

*E-mail: jiangxia@cuhk.edu.hk. Phone: (852) 3943 6165. Fax: (852) 2603 5057.

Notes

The authors declare no competing financial interest.

■ ACKNOWLEDGMENTS

This work was partially funded by an Early Career Scheme grant (No. 404812) and a General Research Fund grant (No. 404413) from the Hong Kong Research Grant Council. This work was also partially supported by the National High Technology Research and Development Program of China (863 Program, 2014AA020521) . This work was inspired by the international and interdisciplinary environments of the JSPS Asian CORE Program, "Asian Chemical Biology Initiative".

■ REFERENCES

(1) Srere, P. A. (1987) Complexes of sequential metabolic enzymes. *Annu. Rev. Biochem. 56*, 89−124.

(2) Hrazdina, G., and Jensen, R. A. (1992) Spatial organization of enzymes in plant metabolic pathways. *Annu. Rev. Plant Physiol. Plant Mol. Biol. 43*, 241−267.

(3) Perham, R. N. (2000) Swinging arms and swinging domains in multifunctional enzymes: catalytic machines for multistep reactions. *Annu. Rev. Biochem. 69*, 961−1004.

(4) Huang, X., Holden, H. M., and Raushel, F. M. (2001) Channeling of substrates and intermediates in enzyme-catalyzed reactions. *Annu. Rev. Biochem. 70*, 149−180.

(5) Agapakis, C. M., Boyle, P. M., and Silver, P. A. (2012) Natural strategies for the spatial optimization of metabolism in synthetic biology. *Nat. Chem. Biol. 8*, 527−535.

(6) Bayer, E. A., Chanzy, H., Lamed, R., and Shoham, Y. (1998) Cellulose, cellulases and cellulosomes. *Curr. Opin. Struct. Biol. 8*, 548−557.

(7) Fontes, C. M. G. A., and Gilbert, H. J. (2010) Cellulosomes: highly efficient nanomachines designed to deconstruct plant cell wall complex carbohydrates. *Annu. Rev. Biochem. 79*, 655−681.

(8) Conrado, R. J., Varner, J. D., and DeLisa, M. P. (2008) Engineering the spatial organization of metabolic enzymes: mimicking nature's synergy. *Curr. Opin. Biotechnol. 19*, 492−499.

(9) Zhang, Y. H. P. (2011) Substrate channeling and enzyme complexes for biotechnological applications. *Biotechnol. Adv. 29*, 715−725.

(10) Fu, J., Liu, M., Liu, Y., and Yan, H. (2012) Spatially-interactive biomolecular networks organized by nucleic acid nanostructures. *Acc. Chem. Res. 45*, 1215−1226.

(11) Hirakawa, H., Haga, T., and Nagamune, T. (2012) Artificial protein complexes for biocatalysis. *Top. Catal. 55*, 1124−1137.

(12) Kim, H., Sun, Q., Liu, F., Tsai, S. L., and Chen, W. (2012) Biologically assembled nanobiocatalysts. *Top. Catal. 55*, 1138−1145.

(13) Schoffelen, S., and van Hest, J. C. M. (2012) Multi-enzyme systems: bringing enzymes together in vitro. *Soft Matter 8*, 1736−1746.

(14) Lee, H., DeLoache, W. C., and Dueber, J. E. (2012) Spatial organization of enzymes for metabolic engineering. *Metab. Eng. 14*, 242−251.

(15) Schoffelen, S., and van Hest, J. C. M. (2013) Chemical approaches for the construction of multi-enzyme reaction systems. *Curr. Opin. Struct. Biol. 23*, 613−621.

(16) Fierobe, H. P., Bayer, E. A., Tardif, C., Czjzek, M., Mechaly, A., Bélaich, A., Lamed, R., Shoham, Y., and Bélaich, J. P. (2002) Degradation of cellulose substrate by cellulosome chimeras. substrate targeting versus proximity of enzyme components. *J. Biol. Chem. 277*, 49621−30.

(17) Mingardon, F., Chanal, A., Tardif, C., Bayer, E. A., and Fierobe, H. P. (2007) Exploration of new geometries in cellulosome-like chimeras. *Appl. Environ. Microbiol. 73*, 7138−49.

(18) Dueber, J. E., Wu, G. C., Malmirchegini, G. R., Moon, T. S., Petzold, C. J., Ullal, A. V., Prather, K. L. J., and Keasling, J. D. (2009) Synthetic protein scaffolds provide modular control over metabolic flux. *Nat. Biotechnol. 27*, 753−759.

(19) You, C., Myung, S., and Zhang, Y. H. P. (2012) Facilitated substrate channeling in a self-assembled trifunctional enzyme complex. *Angew. Chem., Int. Ed. 124*, 8917−8920.

(20) Vong, T., Schoffelen, S., van Dongen, S. F. M., van Beek, T. A., Zuilhof, H., and van Hest, J. C. M. (2011) A DNA-based strategy for dynamic positional enzyme immobilization inside fused silica microchannels. *Chem. Sci. 2*, 1278−1285.

(21) Shimada, J., Maruyama, T., Kitaoka, M., Yoshinaga, H., Nakano, K., Kamiya, N., and Goto, M. (2012) Programmable protein-protein conjugation via DNA-based self-assembly. *Chem. Commun. 48*, 6226−6228.

(22) Fu, J., Liu, M., Liu, Y., Woodbury, N. W., and Yan, H. (2012) Interenzyme substrate diffusion for an enzyme cascade organized on spatially addressable DNA nanostructures. *J. Am. Chem. Soc. 134*, 5516−5519.

(23) Conrad, R. J., Wu, G. C., Boock, J. T., Xu, H., Chen, S. Y., Lebar, T., Turnšek, J., Tomšič, N., Avbelj, M., Gaber, R., Koprivnjak, T., Mori, J., Glavnik, V., Vovk, I., Benčina, M., Hodnik, V., Anderluh, G., Dueber, J. E., Jerala, R., and DeLisa, M. P. (2012) DNA-guided assembly of biosynthetic pathways promotes improved catalytic efficiency. *Nucleic Acids Res. 40*, 1879−89.

(24) Minamihata, K., Goto, M., and Kamiya, N. (2011) Protein heteroconjugation by the peroxidase-catalyzed tyrosine coupling reaction. *Bioconjugate Chem. 22*, 2332−2338.

(25) Grotzky, A., Nauser, T., Erdogan, H., Schluter, A. D., and Walde, P. (2012) A fluorescently labeled dendronized polymer−enzyme conjugate carrying multiple copies of two different types of active enzymes. *J. Am. Chem. Soc. 134*, 11392−11395.

(26) Schoffelen, S., Beekwilder, J., Debets, M. F., Bosch, D., and van Hest, J. C. M. (2013) Construction of a multifunctional enzyme complex via the strain-promoted azide-alkyne cycloaddition. *Bioconjugate Chem. 24*, 987−996.

(27) Srere, P. A., Mattiasson, B., and Mosbach, K. (1973) An immobilized three-enzyme system: a model for microenvironmental compartmentation in mitochondria. *Proc. Natl. Acad. Sci. U. S. A. 70*, 2534−2538.

(28) Peters, R. J. R. W., Marguet, M., Marais, S., Fraaije, M. W., van Hest, J. C. M., and Lecommandoux, S. (2014) Cascade reactions in multicompartmentalized polymersomes. *Angew. Chem., Int. Ed. 53*, 146−150.

(29) Medintz, I. L., Uyeda, H. T., Goldman, E. R., and Mattoussi, H. (2005) Quantum dot bioconjugates for imaging, labelling and sensing. *Nat. Mater. 4*, 435−446.

(30) Algar, W. R., Prasuhn, D. E., Stewart, M. H., Jenning, T. L., Blanco-Canosa, J. B., Dawson, P. E., and Medintz, I. L. (2011) The controlled display of biomolecules on nanoparticles: a challenge suited to bioorthogonal chemistry. *Bioconjugate Chem. 22*, 825−858.

(31) Sapsford, K. E., Algar, W. R., Berti, L., Gemmill, K. B., Casey, B. J., Oh, E., Stewart, M. H., and Medintz, I. L. (2013) Functionalizing nanoparticles with biological molecules: developing chemistries that facilitate nanotechnology. *Chem. Rev. 113*, 1904−2074.

(32) Cedervall, T., Lynch, I., Lindman, S., Berggård, T., Thulin, E., Nilsson, H., Dawson, K. A., and Linse, S. (2007) Understanding the nanoparticle−protein corona using methods to quantify exchange rates and affinities of proteins for nanoparticles. *Proc. Natl. Acad. Sci. U.S.A. 104*, 2050−2055..

(33) Lundqvist, M., Stigler, J., Elia, G., Lynch, I., Cedervall, T., and Dawson, K. A. (2008) Nanoparticle size and surface properties

determine the protein corona with possible implications for biological impacts. *Proc. Natl. Acad. Sci. U.S.A. 105*, 14265−14270.
(34) Walczyk, D., Bombelli, F. B., Monopoli, M. P., Lynch, I., and Dawson, K. A. (2010) What the cell "sees" in bionanoscience. *J. Am. Chem. Soc. 132*, 5761−6768.
(35) Monopoli, M. P., Walczyk, D., Campbell, A., Elia, G., Lynch, I., Bombelli, F. B., and Dawson, K. A. (2011) Physical−chemical aspects of protein corona: relevance to in vitro and in vivo biological impacts of nanoparticles. *J. Am. Chem. Soc. 133*, 2525−2534.
(36) Monopoli, M. P., Åberg, C., Salvati, A., and Dawson, K. A. (2012) Biomolecular coronas provide the biological identity of nanosized materials. *Nat. Nanotechnol. 7*, 779−786.
(37) Lynch, I., de Gregorio, P., and Dawson, K. A. (2005) Simultaneous release of hydrophobic and cationic solutes from thin-film "plum-pudding" gels: a multifunctional platform for surface drug delivery? *J. Phys. Chem. B 109*, 6257−6261.
(38) Clapp, A. R., Medintz, I. L., Mauro, J. M., Fisher, B. R., Bawendi, M. G., and Mattoussi, H. (2004) Fluorescence resonance energy transfer between quantum dot donors and dye-labeled protein acceptors. *J. Am. Chem. Soc. 126*, 301−310.
(39) Sapsford, K. E., Pons, T., Medintz, I. L., Higashiya, S., Brunel, F. M., Dawson, P. E., and Mattoussi, H. (2007) Kinetics of metal-affinity driven self assembly between proteins or peptides and CdSe−ZnS quantum dots. *J. Phys. Chem. C 111*, 11528−11538.
(40) Prasuhn, D. E., Deschamps, J. R., Susumu, K., Stewart, M. H., Boeneman, K., Blanco-Canosa, J. B., Dawson, P. E., and Medintz, I. L. (2010) Polyvalent display and packing of peptides and proteins on semiconductor quantum dots: predicted versus experimental results. *Small 6*, 555−564.
(41) Lu, Y., Wang, J., Wang, J., Wang, L., Au, S. W., and Xia, J. (2012) Genetically encodable design of ligand "bundling" on the surface of nanoparticles. *Langmuir 28*, 13788−92.
(42) Wang, J., Nie, Y., Lu, Y., Liu, J., Wang, J., Fu, A., Liu, T., and Xia, J. (2014) Assembly of multivalent protein ligands and quantum dots: a multifaceted investigation. *Langmuir 30*, 2161−2169.
(43) Bentley, R. (1990) The shikimate pathway-A metabolic tree with many branches. *Crit. Rev. Biochem. Mol. Biol. 25*, 307−384.
(44) Dosselaere, F., and Vanderleyden, J. (2001) A metabolic node in action: chorismate-utilizing enzymes in microorganisms. *Crit. Rev. Microbiol. 27*, 75−131.
(45) Daruwala, R., Kwon, O., Meganathan, R., and Hudspeth, M. E. S. (1996) A new isochorismate synthase specifically involved in menaquinone (vitamin K2) biosynthesis encoded by the menF gene. *FEMS Microbiol. Lett. 140*, 159−163.
(46) Daruwala, R., Bhattacharyya, D. K., Kwon, O., and Meganathan, R. (1997) Menaquinone (Vitamin K2) biosynthesis: Overexpression, purification, and characterization of a new isochorismate synthase from Escherichia coli. *J. Bacteriol. 179*, 3133−3138.
(47) Jiang, M., Cao, Y., Guo, Z.-F., Chen, M., Chen, X., and Guo, Z. (2007) Menaquinone biosynthesis in Escherichia coli: identification of 2-succinyl-5-enolpyruvyl-6-hydroxy-3-cyclohexene-1-carboxylate as a novel intermediate and re-evaluation of MenD activity. *Biochemistry 46*, 10979−89.
(48) Jiang, M., Chen, M., Cao, Y., Yang, Y., Sze, K. H., Chen, X., and Guo, Z. (2007) Determination of the stereochemistry of 2-succinyl-5-enolpyruvyl-6-hydroxy-3-cyclohexene-1-carboxylate, a key intermediate in menaquinone biosynthesis. *Org. Lett. 9*, 4765−7.
(49) Jiang, M., Chen, X., Guo, Z.-F., Cao, Y., Chen, M., and Guo, Z. (2008) Identification and characterization of (1R,6R)-2-succinyl-6-hydroxy-2,4-cyclohexadiene-1-carboxylate synthase in the menaquinone biosynthesis of Escherichia coli. *Biochemistry 47*, 3426−34.
(50) Jiang, M., Chen, X., Wu, X.-H., Chen, M., Wu, Y.-D., and Guo, Z. (2009) Catalytic mechanism of SHCHC synthase in the menaquinone biosynthesis of Escherichia coli: identification and mutational analysis of the active site residues. *Biochemistry 48*, 6921−31.
(51) Kolappan, S., Zwahlen, J., Zhou, R., Truglio, J. J., Tonge, P. J., and Kisker, C. (2007) Lysine 190 is the catalytic base in MenF, the menaquinone-specific isochorismate synthase from Escherichia coli: implications for an enzyme family. *Biochemistry 46*, 946−953.
(52) Dawson, A., Fyfe, P. K., and Hunter, W. N. (2008) Specificity and reactivity in menaquinone biosynthesis: the structure of Escherichia coli MenD (2-succinyl-5-enolpyruvyl-6-hydroxy-3-cyclohexadiene-1-carboxylate synthase). *J. Mol. Biol. 384*, 1353−1368.
(53) Dawson, A., Fyfe, P. K., Gillet, F., and Hunter, W. N. (2011) Exploiting the high-resolution crystal structure of Staphylococcus aureus MenH to gain insight into enzyme activity. *BMC Struct. Biol. 11*, 19−19.
(54) Johnston, J. M., Jiang, M., Guo, Z., and Baker, E. N. (2013) Crystal structures of E. coli native MenH and two active site mutants. *PLoS One 8*, e61325.
(55) Wang, J., and Xia, J. (2011) Preferential binding of a novel polyhistidine peptide dendrimer ligand on Quantum Dots probed by capillary electrophoresis. *Anal. Chem. 83*, 6323−9.
(56) Porath, J., Carlson, J., Olsson, I., and Belfrage, G. (1975) Metal chelate affinity chromatography: a new approach to protein fractionation. *Nature 258*, 598−599.
(57) Miles, E. W., Rhee, S., and Davies, D. R. (1999) The molecular basis of substrate channeling. *J. Biol. Chem. 274*, 12193−6.
(58) Wu, N., Tsuji, S. Y., Cane, D. E., and Khosla, C. (2001) Assessing the balance between protein-protein interactions and enzyme-substrate interactions in the channeling of intermediates between polyketide synthase modules. *J. Am. Chem. Soc. 123*, 6465−74.